Multi-rate sensor fusion-based adaptive discrete finite-time synergetic control for flexible-joint mechanical systems*

Xue Guang-Yue(薛广月)†, Ren Xue-Mei(任雪梅)‡, and Xia Yuan-Qing(夏元清)

School of Automation, Beijing Institute of Technology, Beijing 100081, *China*

(Received 5 February 2013; revised manuscript received 8 April 2013)

This paper proposes an adaptive discrete finite-time synergetic control (ADFTSC) scheme based on a multi-rate sensor fusion estimator for flexible-joint mechanical systems in the presence of unmeasured states and dynamic uncertainties. Multi-rate sensors are employed to observe the system states which cannot be directly obtained by encoders due to the existence of joint flexibilities. By using an extended Kalman filter (EKF), the finite-time synergetic controller is designed based on a sensor fusion estimator which estimates states and parameters of the mechanical system with multi-rate measurements. The proposed controller can guarantee the finite-time convergence of tracking errors by the theoretical derivation. Simulation and experimental studies are included to validate the effectiveness of the proposed approach.

Keywords: adaptive finite-time synergetic control, multi-rate sensor fusion, mechanical systems

PACS: 07.07.Tw, 07.10.–h, 02.30.Yy **DOI:** 10.1088/1674-1056/22/10/100702

1. Introduction

Most servo mechanical systems employ the transmission devices (e.g., gear mechanisms, mechanical spring) which cause nonlinear flexibilities in joints of mechanical systems. However, the challenge of achieving high accuracy and dynamic performance is increased because the nonlinear flexibilities make the states of the mechanical plant not be measured in industrial applications where the actuator measurements, such as the angular position and velocity as well as active motor current, are available only prior to the gear transmission. To find solutions to these challenges, different approaches have been followed for mechanical systems. The sliding mode control (SMC) is an effective approach to design robust controller for dynamic systems with uncertainties found in unmodeled dynamics and external disturbances. Recently, the terminal SMC (TSMC) was used in mechanical system control (e.g. robust TSMC,[1] finite-time control,[2–4] fractional-order SMC[5,6]) since it has some superior properties compared with SMC such as better tracking precision and fast error convergence. In particular, the singularity problem of the TSMC is addressed by Feng[7] and Chai.[8] However, uncertainties of realistic systems derive from incomplete knowledge of the kinematics and dynamics, from join flexibility, actuator dynamics, friction, sensor noise, and unknown loads. In such situations, the SMC necessitates an estimator to be constructed that takes the estimates for states and the uncertainties on the basis of the measurement information.[9]

To estimate states and uncertainties of the flexible-joint mechanical system, many methods, such as neural network (NN) observers,[10,11] extended Kalman filter (EKF),[12] and sliding mode observers,[13] are proposed to estimate link and motor positions/velocities and dynamic parameters in the controller design. In these methods, NN observer-based controllers do not take advantage of motor positions; EKF does not perform better than an adaptive sliding observer when the mechanical system runs at low speeds with heavy loads; EKF has more accurate current tracking ability than the sliding observer for light load systems. Corradinia[14] presented a robust discrete SMC coupled with an uncertainty estimator designed for planar robotic manipulators. For the manipulator system, Islam[15] proposed an output feedback SMC which incorporates a model-free linear observer to estimate unknown velocity signals, but this method is discussed for continuous-time and the plant without joint flexibilities. With the development of computer and electronic technology, modeling and control for mechanical systems have been extensively investigated and many results have been obtained in recent years.[16–19] Yashimura[20] designed an adaptive SMC for an uncertainty discrete-time system using the multi-rate output measurement, however drawbacks of the SMC scheme were not considered, such as the chattering phenomena caused by the high frequency switching control law. Thus the no-chattering SMC has attracted lots of attention for engineering applications.[21] To avoid the chattering phenomena in mechanical system control, the synergetic control (SC) may be a good choice since chatter free operation makes SC a more practical and motivating approach which is easily implementable for digital con-

*Project supported by the National Natural Science Foundation of China (Grant Nos. 61273150 and 60974046) and the Research Fund for the Doctoral Program of Higher Education of China (Grant No. 20121101110029).

†Corresponding author. E-mail: yyyy0225@126.com

‡Corresponding author. E-mail: xmren@bit.edu.cn

© 2013 Chinese Physical Society and IOP Publishing Ltd

trol. SC has been widely utilized in power systems,[22] DC–DC boost converters,[23] and nonlinear systems[24] because it shares with sliding mode control the properties of order reduction and decoupling design procedure. But the finite-time synergetic control (FTSC) is less discussed. Liu proposed the FTSC scheme for robotic manipulators in Ref. [25], however, the issue of digitalization of FTSC scheme and joint flexibilities was not addressed. To the best of our knowledge, few adaptive finite-time synergetic controllers for uncertain flexible-joint mechanical systems using the multi-rate sensor fusion have been presented till now.

To remedy such limitations, this paper proposes a novel adaptive discrete finite-time synergetic control (ADFTSC) based on multi-rate sensor fusion estimator for an uncertain flexible-joint mechanical system. In the method, uncertain parameters and unmeasured states are estimated by an EKF-based fusion estimator which fuses the multi-rate measurements; and the ADFTSC is developed by using the estimates of unmeasured states and uncertainties. The convergence of both the estimation error and the tracking error is proved based on the Lyapunov stability analysis. In the controller scheme, the Euler estimation is also used to estimate the velocity of motor.[26] The effectiveness of the proposed method is indicated by applying it for a two-link flexible-joint manipulator trajectory tracking in simulation and for a turntable visual tracking in experiment.

The main contributions of this work are summarized as follows.

(i) We propose a novel tracking control scheme based on the ADFTSC and the multi-rate sensor fusion estimator for a flexible-joint mechanical system.

(ii) Stability analysis is given by using the Lyapunov method for both the sensor fusion estimator and the controller.

This paper is organized as follows: Section 2 represents the discrete flexible-joint mechanical system model. In Section 3, an adaptive discrete finite-time synergetic controller is presented. A multi-rate sensor data fusion estimator to estimate states and parameters for the flexible-joint mechanical system is presented in Section 4. Stability analysis is given in Section 5. The simulation and experimental studies are implemented in Section 6. The paper ends with conclusion about the proposed approach.

2. Discrete flexible-joint mechanical system model

In this paper, a flexible-joint mechanical system is given with the multi-rate sensors (e.g. joint motor encoders, cameras). The discrete dynamic model of an n-link flexible-joint mechanical system with uncertainties can be obtained as

$$q(k+1) = q(k) + T\dot{q}(k), \tag{1a}$$

$$\dot{q}(k+1) = \dot{q}(k) + M^{-1}(\bar{q},\theta)Tu(k) - F(\bar{q},q,\dot{\bar{q}}_m,\dot{q}_m,T,\theta), \tag{1b}$$

where $q(k)$, $\dot{q}(k)$, and $q_m(k)$, $\dot{q}_m(k)$ denote the position, velocity of the link, and motor angles at k time, respectively; $\bar{q} \cong q(k) + T\dot{q}(k)$, $\dot{\bar{q}}_m = \dot{q}_m(k+1)$, T is the sampling interval; $M(\cdot)$ is the invertible inertia matrix which satisfies $\xi_{\min} \le \|M\| \le \xi_{\max}$,

$$\begin{aligned} &F(\bar{q},q,\dot{\bar{q}}_m,\dot{q}_m,T,\theta) \\ &= M^{-1}(\bar{q},\theta)[M_m(\dot{q}_m(k+1) - \dot{q}_m(k)) + F_m\dot{q}_m(k)] \\ &\quad + M^{-1}(\bar{q}(k),\theta)([M(\bar{q}(k),\theta) - M(q(k),\theta)]\dot{q}(k) \\ &\quad + Tf(q(k),\dot{q}(k)),\theta), \end{aligned}$$

$f(\cdot)$ represents centrifugal, Coriolis, and gravitational forces; M_m and F_m are constant, diagonal, positive-definite matrices representing motor inertia, motor viscous friction, respectively; $u(k)$ denotes the motor torque; the unknown or varying dynamic parameter in the robotic model is defined as $\theta(k)$ which satisfies $\theta(k+1) - \theta(k) = Tw_\theta(k)$.

Define a state vector

$$x(k) = [q(k)^{\mathrm{T}}\ \dot{q}(k)^{\mathrm{T}}]^{\mathrm{T}}.$$

The dynamic in Eq. (1) can be expressed equivalently as a state space representation

$$x(k+1) = Ax(k) + B(k)\tau(k) + \mathbb{F}(k), \tag{2}$$

where

$$A = \begin{bmatrix} I & TI \\ 0 & I \end{bmatrix},\ B(k) = \begin{bmatrix} I & 0 \\ 0 & M^{-1}(\bar{q},\theta)T \end{bmatrix},$$

$$\mathbb{F}(k) = \left[0^{\mathrm{T}}, -F(\bar{q},q,\dot{\bar{q}}_m,\dot{q}_m,T,\theta)^{\mathrm{T}}\right]^{\mathrm{T}},\ \tau(k) = \left[0^{\mathrm{T}}, u(k)^{\mathrm{T}}\right]^{\mathrm{T}}.$$

The multi-rate sensor measurement model is defined as

$$y^i(k) = h^i x(k) + v(k), \tag{3}$$

where $v(k)$ is measurement noise, $i = 1,2$, $i = 1$ denotes the fast sampling rate measurement and $i = 2$ represents the measurement observed by the sensor with slow sampling rate. The sampling rate of different sensors can be given by

$$s_1 = ls_2,$$

where s_1 and s_2 denote the sampling rate of different sensors respectively. l is a positive integer.

The characteristics of multi-rate measurements are shown in Fig. 1 detailedly.

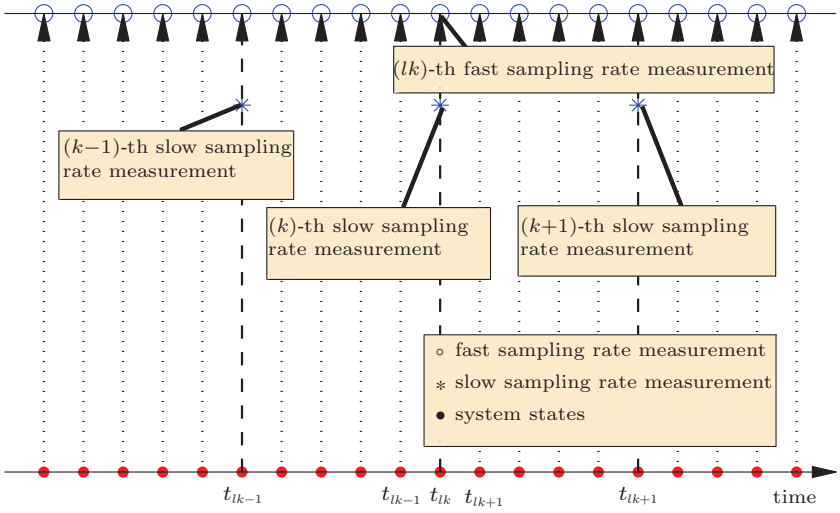


Fig. 1. (color online) The schematic diagram of the relation between multi-rate measurements.

3. Adaptive discrete finite-time synergetic control

3.1. Adaptive discrete finite-time synergetic controller design

In this section, the adaptive discrete finite-time synergetic controller is designed to ensure the tracking of reference variable $x_{\rm d}(k) = [q_{\rm d}(k)^{\rm T}, \dot{q}_{\rm d}(k)^{\rm T}]^{\rm T}$. Here the tracking error $\tilde{x}(k) = x(k) - x_{\rm d}(k)$ is introduced. We define the macrovariable $\sigma(k)$:

$$\sigma(k) = s(\tilde{x}(k)) = S\tilde{x}(k), \tag{4}$$

where S is a constant matrix.

However, in the flexible-joint mechanical system, the state $x(k)$ cannot be measured directly, $\sigma(k)$ is replaced by estimated macrovariable as follows:

$$\hat{\sigma}(k) = s(\hat{x}(k) - x_{\rm d}(k)) = S\varepsilon(k), \tag{5}$$

where $\varepsilon(k) = \varepsilon_{\rm t}(k) - \varepsilon_{\rm e}(k)$, $\varepsilon_{\rm t}(k) = x(k) - x_{\rm d}(k)$ is the tracking error and $\varepsilon_{\rm e}(k) = x(k) - \hat{x}(k)$ denotes the estimation error.

To ensure the tracking error converging at finite-time, an evolution constraint is given by

$$\Lambda[\hat{\sigma}(k+1) - \hat{\sigma}(k)] + T\hat{\sigma}(k)^p = 0, \tag{6}$$

where Λ is the nonsingular positive-definite diagonal matrix, $p = p_1/p_2$, p_1 and p_2 are positive odd numbers and $p \in (1/2, 1)$.

From Eq. (6), we have

$$\hat{\sigma}(k+1) = \hat{\sigma}(k) - \Lambda^{-1}T\hat{\sigma}(k)^p. \tag{7}$$

According to Eqs. (5) and (1), equation (7) can be rewritten with the error dynamic as follows:

$$\begin{aligned} &A\hat{x}(k) + \hat{B}(k)\tau(k) + \hat{\mathbb{F}}(k) - x_{\rm d}(k+1) \\ &= \varepsilon(k) - \Lambda^{-1}TS^{(p-1)}\varepsilon(k)^p, \end{aligned} \tag{8}$$

where $\hat{B}(k)$ and $\hat{\mathbb{F}}(k)$ are given by

$$\hat{B}(k) = \begin{bmatrix} I & 0 \\ 0 & \hat{M}^{-1}(\bar{q},\theta)T \end{bmatrix}, \tag{9}$$

$$\hat{\mathbb{F}}(k) = \left[0^{\rm T}, -\hat{F}(\bar{q}, q, \dot{\bar{q}}_m, \dot{q}_m, T, \theta)^{\rm T}\right]^{\rm T}, \tag{10}$$

where $\hat{M}(\bar{q},\theta)$ and $\hat{F}(\bar{q}, q, \dot{\bar{q}}_m, \dot{q}_m, T, \theta)$ satisfy the following equations

$$\begin{aligned} &M(\bar{q},\theta) \\ &= \hat{M}(\bar{q},\theta) + \Delta M(\bar{q},\theta), \end{aligned} \tag{11}$$

$$\begin{aligned} &F(\bar{q}, q, \dot{\bar{q}}_m, \dot{q}_m, T, \theta) \\ &= \hat{F}(\bar{q}, q, \dot{\bar{q}}_m, \dot{q}_m, T, \theta) + \Delta F(\bar{q}, q, \dot{\bar{q}}_m, \dot{q}_m, T, \theta), \end{aligned} \tag{12}$$

where $\dot{\bar{q}}_m$ denotes $\dot{q}_m(k+1)$; $\hat{M}(\bar{q},\theta) = M(\hat{\bar{q}},\hat{\theta})$ and $\hat{F}(\bar{q}, q, \dot{\bar{q}}_m, \dot{q}_m, T, \theta) = F(\hat{\bar{q}}, \hat{q}, \hat{\dot{\bar{q}}}_m, \hat{\dot{q}}_m, T, \hat{\theta})$ are the estimation of dynamic parameters; $\Delta M(\bar{q},\theta)$ and $\Delta\mathbb{F}(\bar{q}, q, \dot{\bar{q}}_m, \dot{q}_m, T, \theta)$ are bounded variables including the estimation error and system uncertainties,

$$\|\Delta M(\bar{q},\theta)\| \le \delta_{\rm M}, \quad \|\Delta\mathbb{F}(\bar{q}, q, \dot{\bar{q}}_m, \dot{q}_m, T, \theta)\| \le \delta_{\rm F}, \tag{13}$$

with $\delta_{\rm M}$ and $\delta_{\rm F}$ are constants.

By solving Eq. (7), the input $\tau(k)$ is obtained as

$$\begin{aligned} \tau(k) = \hat{B}(k)^{-1}\big[&x_{\rm d}(k+1) - Ax_{\rm d}(k) - \hat{\mathbb{F}}(k) \\ &+ (I-A)\varepsilon(k) - \Lambda^{-1}TS^{p-1}\varepsilon(k)^p\big], \end{aligned} \tag{14}$$

where $\hat{B}(k)$ and $\hat{\mathbb{F}}(k)$ are composed of the estimation of states and dynamic parameters $\hat{\bar{q}}$, $\hat{q}$, $\hat{\dot{\bar{q}}}_m$, $\hat{\dot{q}}_m$, and $\hat{\theta}$ which are obtained by fusion estimator and Euler velocity estimation in the next section. Λ is chosen by

$$\lambda[\Lambda] < \lambda_{\min}[2(S\varepsilon(k))^{1-p}/T], \tag{15}$$

where $\lambda[\bullet]$ denotes the eigenvalue of $\bullet$, especially for the diagonal matrix, it denotes the diagonal elements of matrix.

Remark 1 The major advantage of the proposed controller over the synergetic controller is that the finite-time convergent synergetic control term of controller $-\hat{B}(k)^{-1}\Lambda^{-1}TS^{p-1}\varepsilon(k)^p$ forces the error to zero at finite time.

3.2. Multi-rate sensor fusion estimate

A multi-rate sensor fusion estimate method is designed to take the estimates for the uncertain parameter and states. Defining the augmented vector $z(k) = [x(k)^{\mathrm{T}}, \theta(k)^{\mathrm{T}}]^{\mathrm{T}}$ which is given as

$$z(k+1) = \mathbb{A}(z(k), u(k)) + \Gamma_\theta w(k), \tag{16}$$

$$y_z(k) = h_z^i z(k) + v_z^i(k), \tag{17}$$

where

$$\mathbb{A}(z(k), u(k)) = \begin{bmatrix} Ax(k) + B(k)\tau(k) + \mathbb{F}(k) \\ \theta(k) \end{bmatrix},$$

$$h_z^i = \begin{bmatrix} h_i \\ I \end{bmatrix}, \quad w_(k) = \begin{bmatrix} 0 \\ w_\theta(k) \end{bmatrix}.$$

We assume the process noise $w(k)$ and measurement noise $v_z^i(k)$ are sampled from the independent and identically distributed white Gaussian noise. $w(k)$ and $v_z^i(k)$ satisfy

$$\mathrm{E}\left\{ \begin{bmatrix} w(k) \\ v_z^i(k) \end{bmatrix} \begin{bmatrix} w^{\mathrm{T}}(k) & v_z^{j\mathrm{T}}(k) \end{bmatrix} \right\} = \begin{bmatrix} Q(k) & 0 \\ 0 & R_i(k) \end{bmatrix}, \tag{18}$$

where $\mathrm{E}\{\cdot\}$ denotes the expectation, δ_{ij} is the Kronecker delta function. To implement the extended Kalman filter (EKF), mean and covariance of the initial state are expressed as

$$\mathrm{E}\{z(0)\} = \mu_0, \ \ \mathrm{cov}\{z(0)\} = P_0. \tag{19}$$

As shown in Fig. 1, when $t \neq t_{lk}$, the estimation is calculated by using the fast sampling measurement only, the EKF is competent enough to estimate the state; when $t = t_{lk}$, there are multiple measurements available, the EKF-based weighted measurements fusion estimator is designed to fuse multi-rate datum.

When $t \neq t_{lk}$, we have

$$\hat{z}(k \mid k) = \mathrm{E}\{z(k) \mid Y_k^1\},$$
$$P(k \mid k) = \mathrm{cov}\{z(k) \mid Y_k^1\},$$

where $Y_k^1 = \{y^1(1), y^1(2), \ldots, y^1(k)\}$ represents the set of fast sampling measurements up to time t_k. Using EKF, the estimation at time t_k via fast sampling measurements is given as follows:

$$\hat{z}^-(k \mid k) = \mathbb{A}(\hat{z}(k-1 \mid k-1), u(k)), \tag{20}$$

$$P(k \mid k-1) = A_k P(k-1 \mid k-1) A_k^{\mathrm{T}} + Q(k-1), \tag{21}$$

$$K_k = P(k \mid k-1) h_z^{1\mathrm{T}} [h_z^1 P(k \mid k-1) h_z^{1\mathrm{T}} + R(k)]^{-1}, \tag{22}$$

$$\hat{z}(k \mid k) = \hat{z}^-(k \mid k) + K_k(y^1(k) - h_z^1 \hat{z}^-(k \mid k)), \tag{23}$$

$$P(k \mid k) = (I - K_k h_z^1) P(k \mid k-1), \tag{24}$$

where A_k, W_k are Jacobian matrices and K_k is the correction gain vector. According to the above equations, the estimate and the covariance are updated with the fast sampling rate measurement.

When $t = t_{lk}$ the weighted measurement fusion estimate is given by

$$\hat{z}(k \mid k) = \mathrm{E}\{z(k) \mid Y_k^1, y_k^2\},$$
$$P(k \mid k) = \mathrm{cov}\{z(k) \mid Y_k^1, y_k^2\}.$$

To fuse multiple measurements, we use the weighted least squares (WLS) estimator,

$$y^{[\mathrm{WLS}]}(k) = \left[\sum_{i=1}^{2} h_z^{i\mathrm{T}} R_i^{-1}(k) h_z^i \right]^{-1} \sum_{i=1}^{2} h_z^{i\mathrm{T}} R_i^{-1}(k). \tag{25}$$

Then the weight fusion measurement equation is obtained by

$$y^{[\mathrm{WLS}]}(k) = z(k) + v^{[\mathrm{WLS}]}(k), \tag{26}$$

where the fusion measurement noise $v^{[\mathrm{WLS}]}$ and its covariance are given by

$$v^{[\mathrm{WLS}]}(k) = \left[\sum_{i=1}^{2} h_z^{i\mathrm{T}} R_i^{-1}(k) h_z^i \right]^{-1} \sum_{i=1}^{2} h_z^{i\mathrm{T}} v_i^{-1}(k), \tag{27}$$

$$R^{[\mathrm{WLS}]}(k) = \left[\sum_{i=1}^{2} h_z^{i\mathrm{T}} R_i^{-1}(k) h_z^i \right]^{-1}. \tag{28}$$

Using the fusion measurement given in Eq. (25), the estimate of $z(k)$ at time $t_k = t_{lk}$ can be given in EKF scheme, we have

$$\hat{z}(k \mid k) = \hat{z}^-(k \mid k) + K_k(y^{[\mathrm{WLS}]}(k) - \hat{z}^-(k \mid k)), \tag{29}$$

$$P(k \mid k) = (I - K_k) P(k \mid k-1), \tag{30}$$

$$K_k = P(k \mid k-1)[P(k \mid k-1) + R^{[\mathrm{WLS}]}(k)]^{-1}. \tag{31}$$

The system state $x(k)$ and the parameter $\theta(k)$ can be computed by using the fusion estimator designed in this section. The motor velocity is estimated by using Euler approximation, $\hat{q}_m$ and $\hat{\dot{q}}_m$ are obtained as

$$\hat{\dot{q}}_m \approx \hat{q}_m = [q_m(k) - q_m(k-1)]/T. \tag{32}$$

The Euler velocity estimation is the simplest and most popular method to estimate the motor velocity by using the angular position sample.

4. Stability analysis

Theorem 1 Consider the multiple sensors system given in Eqs. (16), (17), and an EKF-based fusion estimator given in Eqs. (20)–(31), the estimation error is exponentially bounded in mean square.

Proof To verify the stability of the fusion estimator, the Lyapunov function candidate is defined as

$$V_E(k) = \tilde{z}^{\mathrm{T}}(k) P_z^{-1}(k) \tilde{z}(k), \tag{33}$$

where $\tilde{z}(k) = z(k) - \hat{z}(k)$ is the estimation error at time t_k, $P_z(k)$ is the covariance matrix. If $\Delta V_E(k) = V_E(k) - V_E(k-1)$ is always negative except at $\tilde{z}(k) = 0$ as k increases, $\tilde{z}(k)$ converges to zero. Using Eqs. (20)–(31), $\Delta V_E(k)$ is evaluated as

$$\begin{aligned}
\Delta V_E(k) &= V_E(k) - V_E(k-1) \\
&= \tilde{z}^{\mathrm{T}}(k) P_z^{-1}(k) \tilde{z}(k) - \tilde{z}^{\mathrm{T}}(k-1) P_z^{-1}(k-1) \tilde{z}(k-1) \\
&= \tilde{z}^{\mathrm{T}}(k) \left[(I - K_k h_z^1)(A_k P(k-1) A_k^{\mathrm{T}}) \right]^{-1} \tilde{z}(k) \\
&\quad - \tilde{z}^{\mathrm{T}}(k-1) P_z^{-1}(k-1) \tilde{z}(k-1) \\
&\approx \tilde{z}^{\mathrm{T}}(k-1) A_k^{\mathrm{T}} \left[(I - K_k h_z^1)(A_k P(k-1) A_k^{\mathrm{T}}) \right]^{-1} \\
&\quad \times A_k \tilde{z}(k-1) - \tilde{z}^{\mathrm{T}}(k-1) P_z^{-1}(k-1) \tilde{z}(k-1) \\
&= -\tilde{z}^{\mathrm{T}}(k-1) \left[K_k h_z^1 (A_k P(k-1)) \right]^{-1} A_k \tilde{z}(k-1) \\
&= -\tilde{z}^{\mathrm{T}}(k-1) [P(k \mid k-1) h_z^{1\mathrm{T}} (h_z^1 P(k \mid k-1) h_z^{1\mathrm{T}} \\
&\quad + R(k))^{-1} h_z^1 (A_k P(k-1))]^{-1} A_k \tilde{z}(k-1) \\
&= -\tilde{z}^{\mathrm{T}}(k-1) [A_k P(k-1) A_k^{\mathrm{T}} h_z^{1\mathrm{T}} (h_z^1 A_k P(k-1) A_k^{\mathrm{T}} h_z^{1\mathrm{T}} \\
&\quad + R(k))^{-1} h_z^1 (A_k P(k-1))]^{-1} \times A_k \tilde{z}(k-1) \\
&= -\tilde{z}^{\mathrm{T}}(k-1) [I + P^{-1}(k-1) A_k^{-1} h_z^{1\mathrm{T}} \\
&\quad \times R(k-1) (h_z^1)^{-\mathrm{T}} A_k^{-\mathrm{T}}] P(k-1) \tilde{z}(k-1),
\end{aligned} \tag{34}$$

where $\left[I + P^{-1}(k-1) A_k^{-1} h_z^{1\mathrm{T}} R(k-1) h_z^{1-\mathrm{T}} A_k^{-\mathrm{T}} \right] P(k-1)$ is positive-definite matrix with the eigenvalue γ, we have

$$\Delta V_E(k) \leq -\gamma \parallel \tilde{z}(k-1) \parallel^2 \leq 0. \tag{35}$$

Theorem 2 Consider the rigid-link flexible-joint manipulators system described by Eq. (2), the control law given in Eq. (14) can make the tracking error converge exponentially asymptotically approach zero depending on the parameter Λ.

Proof The Lyapunov method is used to analyze the stability of the EKF-based fusion estimator.[26] In this paper, the proof chooses a Lyapunov candidate defined as

$$V_T(k) = \varepsilon(k)^{\mathrm{T}} \varepsilon(k). \tag{36}$$

The time difference of $V_T(k)$ can be given by

$$\begin{aligned}
\Delta V_T(k+1) &= V_T(k+1) - V_T(k) \\
&= \varepsilon(k+1)^{\mathrm{T}} \varepsilon(k+1) - \varepsilon(k)^{\mathrm{T}} \varepsilon(k),
\end{aligned} \tag{37}$$

where $\varepsilon(k+1) = \hat{x}(k+1) - x_{\mathrm{d}}(k+1)$. From Eqs. (7), (8), and (14), we have

$$\begin{aligned}
\Delta V_T(k+1) &= (\varepsilon(k) - \Lambda^{-1} T S^{p-1} \varepsilon(k)^p)^{\mathrm{T}} (\varepsilon(k) \\
&\quad - \Lambda^{-1} T S^{p-1} \varepsilon(k)^p) - \varepsilon(k)^{\mathrm{T}} \varepsilon(k).
\end{aligned} \tag{38}$$

For simplicity, here we use the notation $\underline{\Lambda}$ instead of $\Lambda^{-1} T S^{p-1}$, then equation (38) can be expressed as

$$\begin{aligned}
&\Delta V_T(k+1) \\
&= (\varepsilon(k) - \underline{\Lambda} \varepsilon(k)^p)^{\mathrm{T}} (\varepsilon(k) - \underline{\Lambda} \varepsilon(k)^p) - \varepsilon(k)^{\mathrm{T}} \varepsilon(k) \\
&= -\varepsilon(k)^{\mathrm{T}} \underline{\Lambda} \varepsilon(k)^p - (\varepsilon(k)^p)^{\mathrm{T}} \underline{\Lambda}^{\mathrm{T}} \varepsilon(k) + (\varepsilon(k)^p)^{\mathrm{T}} \underline{\Lambda}^{\mathrm{T}} \underline{\Lambda} \varepsilon(k) \\
&= -(\varepsilon(k)^p)^{\mathrm{T}} \left[(\varepsilon(k)^{1-p})^{\mathrm{T}} \underline{\Lambda} + \underline{\Lambda} \varepsilon(k)^{1-p} - \underline{\Lambda}^{\mathrm{T}} \underline{\Lambda} \right] \\
&\quad \times \varepsilon(k)^p.
\end{aligned} \tag{39}$$

When Λ is chosen as shown in Eq. (15), we have

$$\begin{aligned}
\Delta V_T(k+1) &= \left(\lambda[\Lambda] - \lambda_{\min}[2(S\varepsilon(k))^{1-p}/T] \right) \| \varepsilon(k)^p \|^2 \\
&< 0.
\end{aligned} \tag{40}$$

The inequality (40) indicates that the proposed controller guarantees the stability of the flexible-joint mechanical system (1).

5. Simulation and experimental studies

5.1. Simulation study

The results obtained from the simulation of the proposed control scheme on a two-link RLFJ manipulator are shown in this section. In the simulation, the aim is to make the RLFJ manipulator whose kinematics parameters are shown in Fig. 2 track desired trajectories $q_{1d} = (25 - 28\mathrm{e}^{-t} + 7\mathrm{e}^{-4t})/20$ and $q_{2d} = (5 + 4\mathrm{e}^{-t} - \mathrm{e}^{-4t})/4$ from the initial position $[q_{1i}, q_{2i}] = [1, 1.5]$. Robotic dynamic parameters are given by

$$M(q) = \begin{bmatrix} (m_1+m_2) l_1^2 + m_2 l_2^2 + 2 m_2 l_1 l_2 \cos(q_2) & m_2 l_2^2 + m_2 l_1 l_2 \cos(q_2) \\ m_2 l_2^2 + m_2 l_1 l_2 \cos(q_2) & m_2 l_2^2 \end{bmatrix},$$

$$g(q) = \begin{bmatrix} -(m_1+m_2) g l_1 \sin(q_1) - m_2 g l_2 \sin(q_1+q_2) \\ -m_2 g l_2 \sin(q_1+q_2)) \end{bmatrix}, \quad C = \begin{bmatrix} -m_2 l_1 l_2 \sin(q_2)(2\dot{q}_1 \dot{q}_2 + \dot{q}_2^2) \\ -m_2 l_1 l_2 \sin(q_2) \dot{q}_1 \dot{q}_2, \end{bmatrix},$$

where m_i and l_i are given in Table 1. For $i = 1,2$, m_i, and l_i denote mass and length of the i-th link.

$$k_m = \mathrm{diag}\{10,10\}\ \mathrm{Nm/rad}, \quad M_m = \mathrm{diag}\{0.5,0.5\}\ \mathrm{kg\cdot m^2},$$

and $F_m = \mathrm{diag}\{4,0.5\}$ Nm·s/rad.

In order to demonstrate the tracking performance, a DTSMC controller is also simulated whose control law is given by

$$u(k) = \frac{\hat{M}}{T}\left[\hat{\mathbb{F}} + \left(\dot{q}_\mathrm{d}(k) - \dot{q}_\mathrm{d}(k-1) + \lambda\tilde{q}_\mathrm{t}(k) + \tilde{q}_\mathrm{t}(k)\right]^p\right] - hs(k) - \zeta(k)\mathrm{sgn}(s(k)),$$

with a sliding surface $s(k) = \dot{\tilde{q}}_\mathrm{t}(k) + \lambda\tilde{q}_\mathrm{t}(k)^p$.

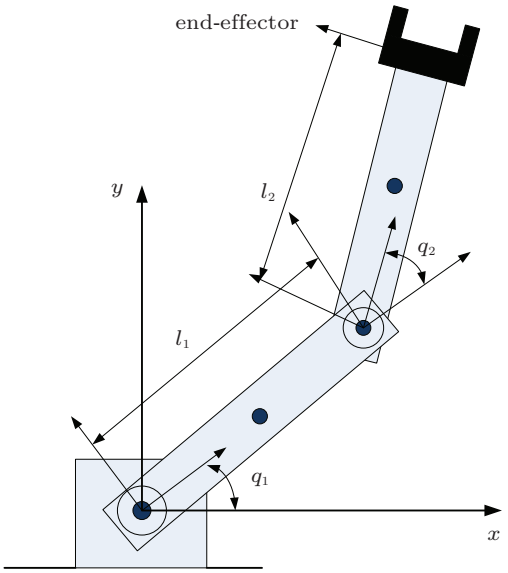


Fig. 2. The schematic drawing of a robotic manipulator with kinematics parameters.

Table 1. Parameters of the 2-DOF manipulator.

link$_i$	m_i/kg	l_i/cm	q_i
1	2.5	35	$q_1(0^\circ \sim 180^\circ)$
2	3	25	$q_2(-160^\circ \sim 160^\circ)$

Parameters of the proposed controller and DTSMC are selected as: $T = 0.01$ s, $h = \mathrm{diag}\{2,2\}$, $\lambda = \mathrm{diag}\{1.5,1.5\}$, $\Lambda = \mathrm{diag}\{2,2\}$, $\zeta = \mathrm{diag}\{25,25\}$, and $p_1 = 3$, $p_2 = 5$. $\theta(k) = 0.05$ is chosen as a constant model parameter whose initial value is $\theta(0) = 0$, and initial values of states for tracking controller are given by $x(0) = [q_1(0), q_2(0)]^\mathrm{T} = [1, 1.5]^\mathrm{T}$, $\dot{x}(0) = [\dot{q}_1(0), \dot{q}_2(0)]^\mathrm{T} = [0,0]^\mathrm{T}$. The initial values of states fusion estimator are given as $x(0) = [q_1(0), q_2(0)]^\mathrm{T} = [0.8, 1.6]^\mathrm{T}$, $\dot{x}(k) = [\dot{q}_1(0), \dot{q}_2(0)]^\mathrm{T} = [0,0]^\mathrm{T}$, $Q(k) = 0.01I$, $R(k) = 0.05I$.

As shown in Figs. 3 and 4, the multi-rate measurements with Gaussian noise and the estimation of joint position are plotted, and the velocity estimation of joints is given in Figs. 5 and 6. Estimation errors of position, velocity and parameter are shown in Fig. 7. The comparative performance of trajectory tracking of joints by using the proposed method and DTSMC is shown in Fig. 8, the tracking error is plotted in details in Fig. 9. Figure 10 plots the input control. It is seen from Fig. 7 that the estimate errors of the state and the unknown parameter almost converge to zero in a short time, and the effect of the measurement noise almost disappears as time increases. In conclusion, simulation results clearly indicate the effectiveness of the proposed approach.

5.2. Experimental study

To demonstrate the applicability of the proposed method, a turntable motor servo system with a camera is employed as the experimental plant (Fig. 10), which consists of a servo motor (PMSM, HC-UFS13) with an encoder and a motor-drive card (MRJ2S10A), a digital controller (DSP, TMS3202812), and a host PC Pentium IV 2.8 GHz PC. This plant is used to implement the point-to-point tracking control, where the servo motor is operated in direct torque control mode.

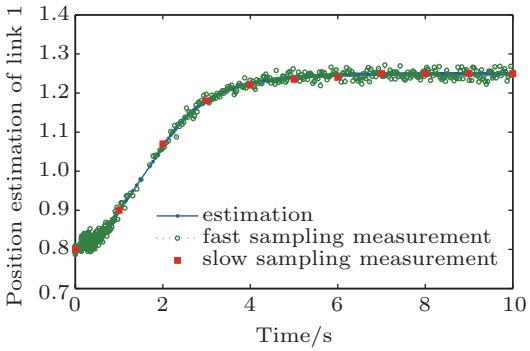


Fig. 3. (color online) The position estimation of link 1.

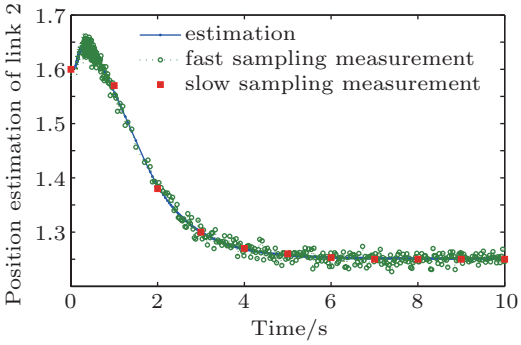


Fig. 4. (color online) The position estimation of link 2.

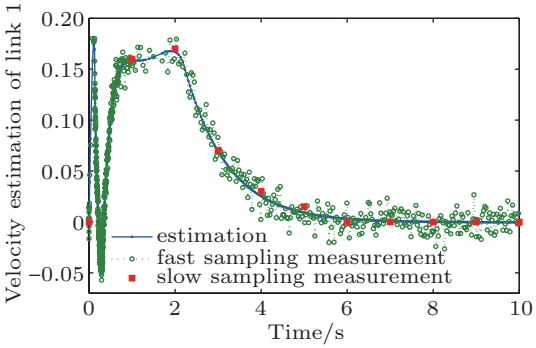


Fig. 5. (color online) The velocity estimation of link 1.

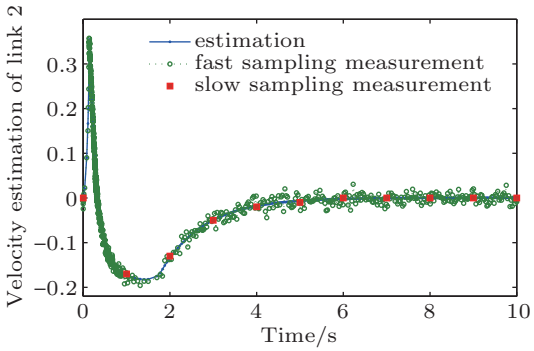


Fig. 6. (color online) The velocity estimation of link 2.

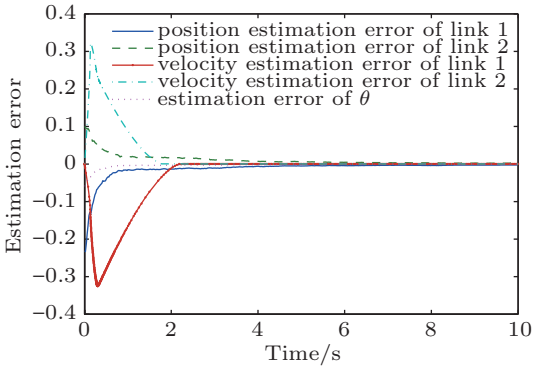


Fig. 7. (color online) Estimation errors.

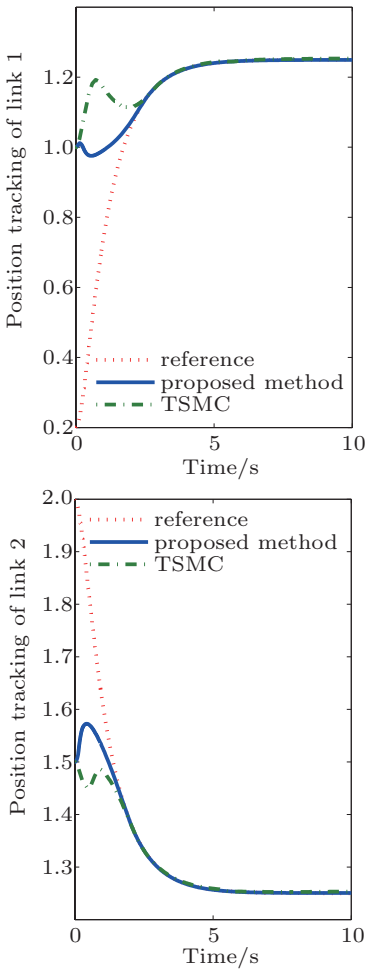


Fig. 8. (color online) Position tracking trajectories of joints.

In the test, the angular position of motor is measured by using an encoder with a resolution of 800 divisions, and the quadrature encoder pulse (QEP) circuit is used for capturing and converting the speed and position information of the turntable encoders. A gear transmission system with a gear ratio of 80 is included, then the encoder output signals have a resolution of $800 \times 80 = 64000$ per rotation. Since the gear mechanism exists, the position of motor is not exactly equivalent to the position of plant. Therefore, a camera is used to measure the angular of the plant by computing the distance between center of the optical axis and reference maker in the image space (Fig. 10), but the sampling rate of camera is slow. To take full advantage of these multi-rate sensors, we design an estimator by fusing the motor position measurements and camera measurements. In the experiments, only yaw axis is used, a sampling rate of 0.01 s is selected for encoder and controller, and a sampling rate of 0.1 s is selected for the camera. Parameters turntable are given: the mass of the plant $m_1 = 20$ kg; the diameter of the plant $l_1 = 0.5$ m, the measurement errors are $\Delta l_1 = 0.05$ m, $\Delta m_1 = 0.1$ kg.

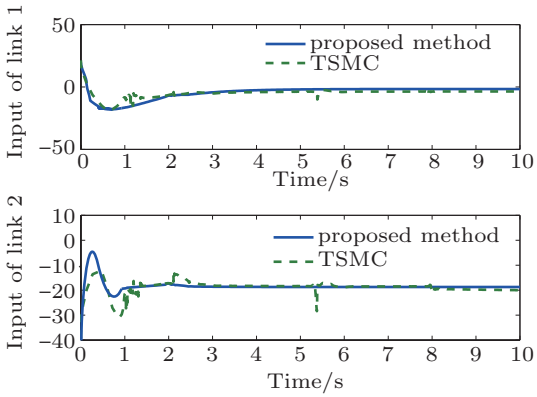


Fig. 9. (color online) Control inputs.

Camera measurements are obtained from the image sequences (Fig. 11) according to the coordinate relation of Cartesian and image shown in Fig. 10. Define the position in the image coordinate $y(k) = [x_m(k), y_m(k)]$ as given in Fig. 11, and the position in the Cartesian coordinate $r(k) = [x_c(k), y_c(k)]$, we calculate the mapping from joint space to image space by using the pinhole camera model, as follows:

$$\frac{f}{H_c - f}\begin{bmatrix} x_m(k) \\ y_m(k) \end{bmatrix} = \begin{bmatrix} x_c(k) \\ y_c(k) \end{bmatrix},$$

where H_c is the perpendicular distance between the camera and the reference plane, f denotes the focal length of the camera. According to the above equation, the joint position can be obtained by calculating the inverse circular trigonometric functions $\arccos[x_m(k)f/(l_1(H_c - f))]$. Vision measurements are converted to joints measurements which are shown in Fig. 12.

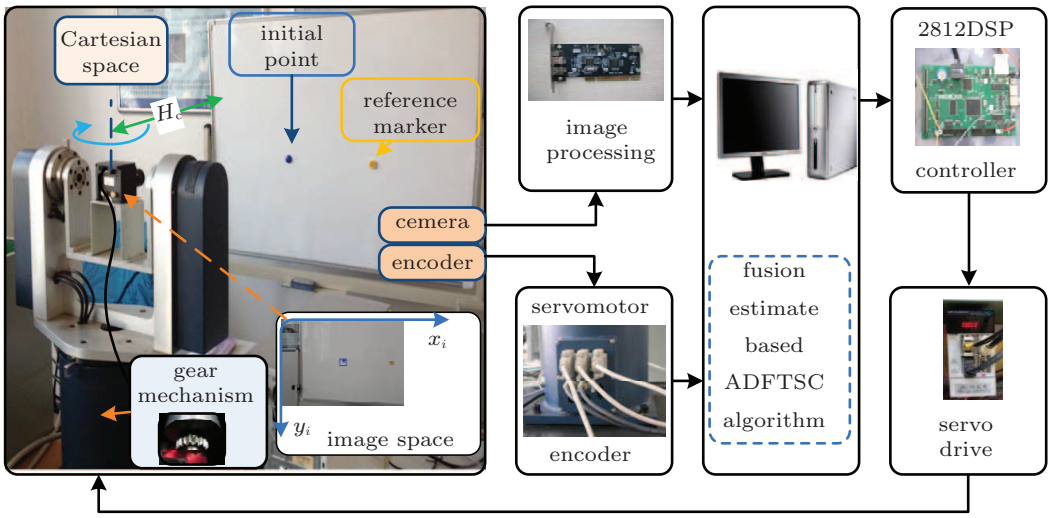


Fig. 10. (color online) Experiment setup and the coordinate relation of Cartesian space and image space.

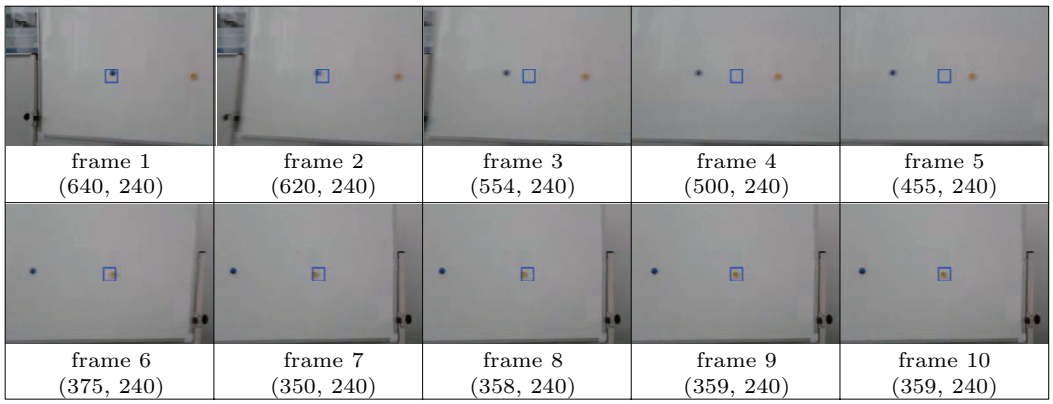


Fig. 11. (color online) The image sequences of 10 frames and the pixel information of reference marker.

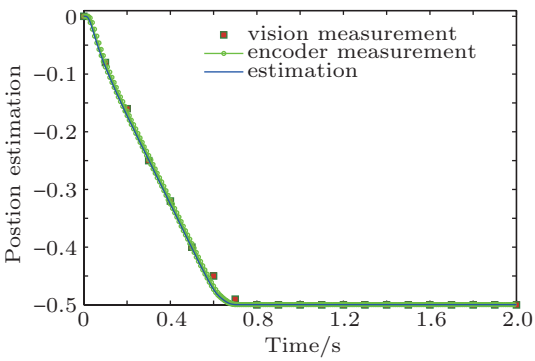


Fig. 12. (color online) The position estimation.

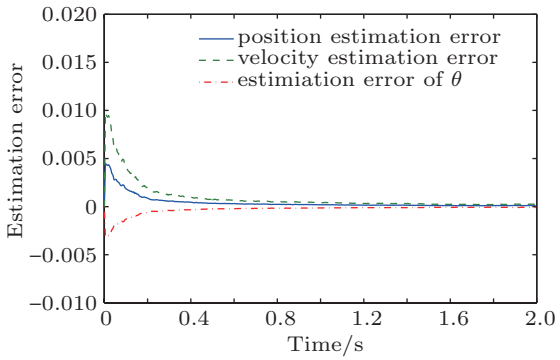


Fig. 13. (color online) Estimation errors.

In the experiment, camera parameters are $f = 0.035$ m, 720×480 pixels, $H_c = 1.5$ m. Parameters of DTSMC and proposed controller are selected as: $T = 0.01$ s, $h = 3$, $\lambda = 2$, $\Lambda = 1.5$, $S = 1$, $\theta(k) = 0.05$; $p = 3$, $q = 5$, $\delta_M = 0.2$, and $\delta_F = 2$. The position of plant is estimated by using multi-rate measurements which are plotted in Fig. 12 with the position estimation. In the test, the velocity of the plant is computed based on the Euler estimation. Estimation errors of both plant's states and the parameter θ are shown in Fig. 13. The tracking controller is designed based on discrete-time synergetic control and states estimation. According to the comparative position tracking performances shown given in Fig. 14, it is obvious that the proposed controller provides a superior behavior.

6. Conclusion

This paper proposes a novel tracking controller based on ADFTSC and multi-rate sensor fusion estimation for flexible-joint mechanical systems. States and uncertainties of the

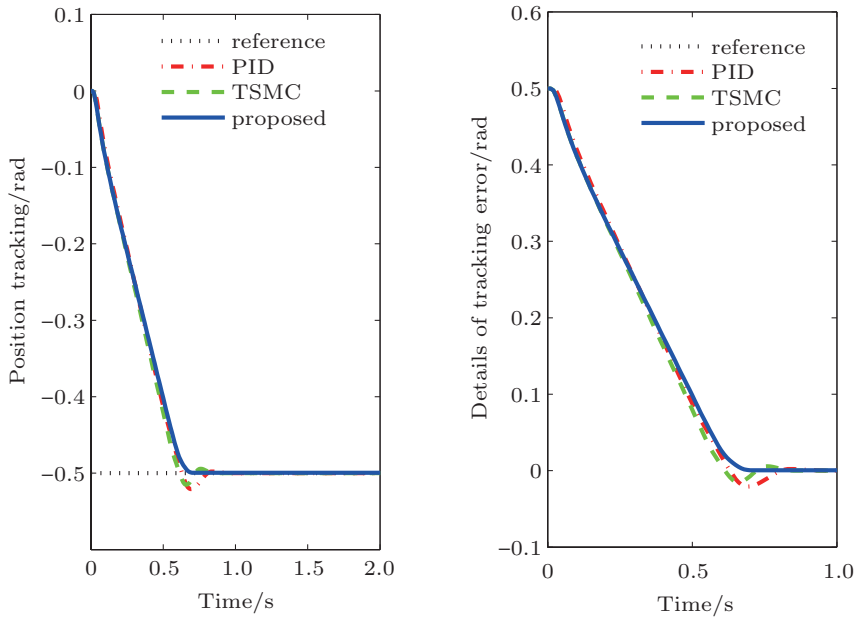


Fig. 14. (color online) Comparative tracking performance

mechanical system are estimated by an EKF-based sensor fusion algorithm which combines multi-rate measurements from multiple sensors. The Lyapunov method is used to verify that both estimation error and tracking error are convergent. The effectiveness of proposed approach is shown in simulation and experiment studies.

References

[1] Yu S, Yu X, Shirinzadeh B and Man Z 2005 *Automatica* **41** 1957
[2] Gao T, Chen Z, Yuan Z and Chen G 2006 *Chin. Phys.* **15** 1190
[3] Mohammad A and Hassan F 2012 *Chin. Phys. B* **21** 060506
[4] Mohammad A 2011 *Chin. Phys. B* **20** 090505
[5] Chen D, Zhang R and Ma X 2012 *Chin. Phys. B* **21** 120507
[6] Abidi K, Xu J and She J 2009 *IEEE T. Ind. Electron.* **56** 3619
[7] Feng Y, Xu X and Man Z 2002 *Automatica* **38** 2159
[8] Wang L, Chai T and Zhai L 2009 *IEEE T. Ind. Electron.* **56** 3296
[9] Yoshimura T 2010 *J. Vib. Control* **16** 1417
[10] Abdollahi F, Talebi H A and Rajnikant V P 2006 *IEEE T. Neural Network* **17** 118
[11] Na J, Ren X and Zheng D 2012 *IEEE T. Neural Network Learn. Syst.*
[12] Lightcap C A and Banks S A 2010 *IEEE T. Control System Tech.* **56** 91
[13] Xu Z and Rahman M F 2012 *IEEE T. Ind. Electron.* **59** 4179
[14] Corradinia M L, Fossib V, Giantomassib A, Ippolitib G, Longhib S and Orlandob G 2012 *Control Eng. Pract.* **20** 816
[15] Islam S and Liu P X 2010 *Robotica* **28** 975
[16] Zhang H B, Lü H S and Gu S L 2010 *Acta Phys. Sin.* **59** 5213 (in Chinese)
[17] Wang J, Xia L and Hou Q 2006 *Chin. Phys.* **15** 467
[18] Zhang H 2002 *Chin. Phys.* **11** 1
[19] Wang J, Hui G and Xie X 2013 *Chin. Phys. B* **22** 030206
[20] Yoshimura T 2012 *Int. J. Syst. Sci.* **43** 211
[21] Chen D, Liu Y and Ma X 2011 *Chin. Phys. B* **20** 120506
[22] Santi E, Monti A, Li D, Proddutur K and Dougal R A 2004 *J. Circ. Syst. Comput.* **13** 737
[23] Jiang Z and Dougal R A 2004 *IEEE T. Power Electron.* **19** 1140
[24] Crossley N 2008 *J. Guid. Control Dyn.* **31** 1561
[25] Liu C and Hsiao M 2012 *Comput. Math. Appl.* **64** 1163
[26] Veselic B, Perunicic-Drazenovic B and Milosavljevic C 2010 *IEEE T. Ind. Electron.* **57** 3840
[27] Kluge S, Reif K and Brokate M 2010 *IEEE T. Automat. Control* **55** 514